Available online at www.sciencedirect.com
ScienceDirect
Journal of Sound and Vibration 304 (2007) 625–639
JOURNAL OF SOUND AND VIBRATION
www.elsevier.com/locate/jsvi

Distributed signal analysis of free-floating paraboloidal membrane shells

H.H. Yue[a,*], Z.Q. Deng[a], H.S. Tzou[b]

[a]School of Mechatronic Engineering, Harbin Institute of Technology, Harbin 150001, China
[b]Department of Mechanical Engineering, StrucTronics Lab, University of Kentucky, Lexington, KY 40506-0503, USA

Received 9 February 2006; received in revised form 3 October 2006; accepted 4 March 2007

Abstract

Multifarious thin paraboloidal shell structures with unique geometric characteristics are utilized in aerospace, telecommunication and other engineering applications over the years. Governing equations of motion of paraboloidal shells are complicated and closed-form analytical solutions of these partial differential equations (PDEs) are difficult to derive. Furthermore, distributed monitoring technique and its resulting global sensing signals of thin flexible membrane shells are not well understood. This study focuses on spatially distributed modal sensing characteristics of free-floating flexible paraboloidal membrane shells laminated with distributed sensor patches based on a new set of assumed mode shape functions. In order to evaluate overall sensing/control effects, microscopic sensing signal characteristic, sensor segmentation and location of distributed sensors on thin paraboloidal membrane shells with different curvatures are investigated. Parametric analysis suggests that the signal generation depends on modal membrane strains in the meridional and circumferential directions in which the latter is more significant than the former, while all bending strains vanish in membrane shells. This study (1) demonstrates an analysis method for distributed sensors laminated on lightweight paraboloidal flexible structures and (2) identifies critical components and regions that generate significant signals for various shell modes.

1. Introduction

Distributed sensor and control of shell structures based on the smart material and structronics technology has been quickly developed in the last 20 years. Smart structures and structronic system are widely used in the field of active shape and vibration control of high performance structures, and detailed reviews of the state of smart structure technologies are provided [1–3]. More smart materials are applied to measurement and control of fully integrated devices or systems, e.g., piezoelectric, shape memory materials, photostrictive materials, electrorheological fluid (ER) and magnetorheological fluid (MR), etc. [4–6]. Because the piezoelectric material exhibits both direct and converse piezoelectric effects, it can serve as distributed sensor and actuator for structural health monitoring and precision control [7].

*Corresponding author. Tel./fax: +86 0451 86413857.
E-mail address: block@hit.edu.cn (H.H. Yue).

0022-460X/$ - see front matter © 2007 Elsevier Ltd. All rights reserved.
doi:10.1016/j.jsv.2007.03.018

Paraboloidal shells of revolution are often used as key components in many advanced aerospace structures and mechanical systems, such as nozzles, antennas, reflectors, rocket fairings, etc. To research methods of exact control and sense of double curvature shells, a large number of investigations have been carried out over the years. Independent modal control of flexible rings using orthogonal convolving piezoelectric sensors and actuators was studied [8]. Distributed excitation and control of cylindrical shells with fully distributed actuator, partially distributed actuators, segmented actuator patches, line actuators, etc. were also studied [9,10]. Distributed sensing and control of shallow spherical shells have been investigated in the past few years [11]. Micro-signals of conical shells and shell panels were evaluated [12]. Distributed modal voltages and their spatial strain characteristics of toroidal shells and spherical shells were recently investigated [13,14]. Spatially distributed sensing of paraboloidal shell based on the bending approximation theory was studied recently [15]. However, distributed sensing and control of flexible paraboloidal shells and their applications to micro and large precision optical and antenna structures are still lacking and need to be fully explored. Based on a new set of mode shape function, this study is to investigate modal dependent spatially distributed sensing signal of lightweight membrane shells of revolution, and to evaluate the factors that influence the effects of sensing signals, e.g., shell curvature, sensor segment locations and major signal components.

2. Modeling of flexible paraboloidal shells

A generic paraboloidal shell of revolution is placed in a tri-orthogonal global coordinate system (X, Y, Z) and the shell itself is defined in a tri-orthogonal curvilinear coordinate system (ϕ,ψ,α_3), shown in Fig. 1. Two radii of the double curvatures, respectively, are R_ϕ and R_ψ; ϕ denotes angular change in the meridian direction and ψ denotes angular change in the circumferential direction. The Lamé parameters of the shell are $A_1 = R_\phi$ and $A_2 = R_\phi \sin\phi$.

If there are no large rotations involved in shell dynamics, the effects of rotary inertias can be neglected in thin shells. Also the transverse shear deformations are not considered in thin shells. Thus, fundamental equation of paraboloidal shell can be derived. Substituting the parameters into the generic shell equation and simplifying yields the fundamental system equations of paraboloidal shell [7]:

$$\frac{\partial(R_\psi N_{\phi\phi}\sin\phi)}{\partial\phi} + R_\phi\frac{\partial N_{\psi\phi}}{\partial\psi} - N_{\psi\psi}R_\phi\cos\phi + R_\phi R_\psi\sin\phi\left(\frac{Q_{\phi 3}}{R_\phi} + F_1\right) = R_\phi R_\psi\sin\phi\rho h\ddot{u}_\phi, \tag{1}$$

$$\frac{\partial(R_\psi N_{\phi\psi}\sin\phi)}{\partial\phi} + R_\phi\frac{\partial N_{\psi\psi}}{\partial\psi} - N_{\psi\phi}R_\phi\cos\phi + R_\phi R_\psi\sin\phi\left(\frac{Q_{\psi 3}}{R_\psi} + F_2\right) = R_\phi R_\psi\sin\phi\rho h\ddot{u}_\psi, \tag{2}$$

$$\frac{\partial(R_\psi Q_{\phi 3}\sin\phi)}{\partial\phi} + R_\phi\frac{\partial Q_{\psi 3}}{\partial\psi} - R_\phi R_\psi\sin\phi\left(\frac{N_{\phi\phi}}{R_\phi} + \frac{N_{\psi\psi}}{R_\psi}\right) + R_\phi R_\psi\sin\phi F_3 = R_\phi R_\psi\sin\phi\rho h\ddot{u}_3, \tag{3}$$

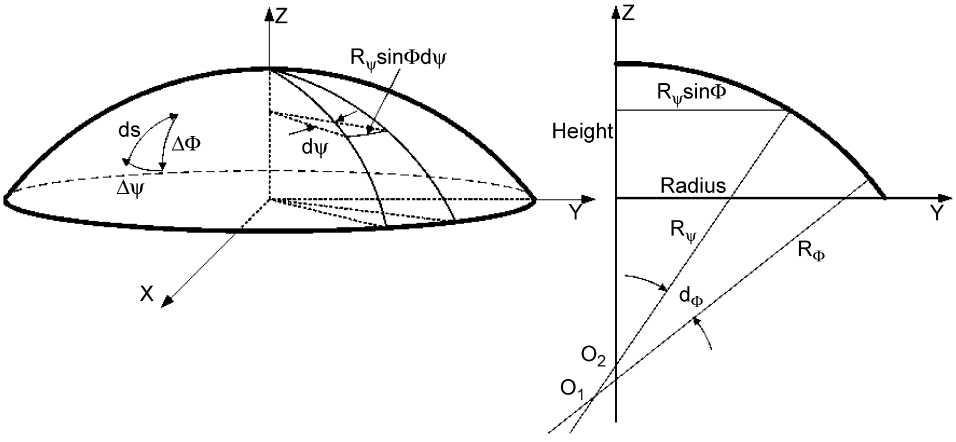

Fig. 1. Definition of a generic paraboloidal shell.

where

$$Q_{\phi 3} = \frac{1}{R_\phi R_\psi \sin\phi}\left[\frac{\partial(M_{\phi\phi} R_\psi \sin\phi)}{\partial\phi} + R_\phi \frac{\partial M_{\psi\phi}}{\partial\psi} - M_{\psi\psi} R_\phi \cos\phi\right], \tag{4}$$

$$Q_{\psi 3} = \frac{1}{R_\phi R_\psi \sin\phi}\left[\frac{\partial(M_{\psi\phi} R_\psi \sin\phi)}{\partial\phi} + R_\phi \frac{\partial M_{\psi\psi}}{\partial\psi} - M_{\psi\phi} R_\phi \cos\phi\right]. \tag{5}$$

Here ρ is the shell mass density; h is the thickness of shell; F_1, F_2 and F_3, respectively are the input forces in the meridional, circumferential and transverse directions; $\ddot{u}_i$ is the acceleration in the ith direction. Note that the radii of curvatures $R_\phi = b/\cos^3\phi$ and $R_\psi = b/\cos\phi$. Imposing the Kirchhoff–Love assumptions and neglecting the twisting in-plane effect of shells, the membrane strains $s_{33} = s_{\phi 3} = s_{\psi 3} = 0$ and other membrane and bending strains are defined as follows:

$$s^o_{\phi\phi} = \frac{\cos^3\phi}{b}\left(\frac{\partial u_\phi}{\partial\phi} + u_3\right), \tag{6}$$

$$s^o_{\psi\psi} = \frac{\cos\phi}{b\sin\phi}\left(\frac{\partial u_\psi}{\partial\psi} + u_\phi\cos\phi + u_3\sin\phi\right), \tag{7}$$

$$s^o_{\phi\psi} = \frac{\cos\phi}{b\sin\phi}\left(\frac{\partial u_\phi}{\partial\psi} + \cos^2\phi\sin\phi\frac{\partial u_\psi}{\partial\phi} - u_\psi\cos\phi\right), \tag{8}$$

$$k_{\phi\phi} = \frac{\cos^6\phi}{b^2}\left(\frac{\partial u_\phi}{\partial\phi} - \frac{\partial^2 u_3}{\partial\phi^2}\right) - \frac{3\cos^5\phi\sin\phi}{b^2}\left(u_\phi - \frac{\partial u_3}{\partial\phi}\right), \tag{9}$$

$$k_{\psi\psi} = \frac{\cos^2\phi}{b^2\sin\phi}\left(\frac{\partial u_\psi}{\partial\psi} - \frac{1}{\sin\phi}\frac{\partial^2 u_3}{\partial\psi^2} + u_\phi\cos^3\phi - \cos^3\phi\frac{\partial u_3}{\partial\phi}\right), \tag{10}$$

$$k_{\phi\psi} = \frac{\cos^4\phi}{b^2\sin\phi}\frac{\partial u_\phi}{\partial\psi} - \frac{2\cos^4\phi}{b^2\sin\phi}\frac{\partial u_3}{\partial\psi\partial\phi} + \frac{\cos^4\phi}{b^2}\frac{\partial u_\psi}{\partial\phi} + \frac{2\cos^3\phi}{b^2\sin^2\phi}\frac{\partial u_3}{\partial\psi} - \left(\frac{\cos^5\phi + 2\cos^3\phi\sin^2\phi}{b^2\sin\phi}\right)u_\psi. \tag{11}$$

Using the relations between the mechanical force and stress, one can derive the mechanical membrane forces and bending moments for thin shells:

$$N_{\phi\phi} = K(s^o_{\phi\phi} + \mu s^o_{\psi\psi}), \tag{12}$$

$$N_{\psi\psi} = K(s^o_{\psi\psi} + \mu s^o_{\phi\phi}), \tag{13}$$

$$N_{\phi\psi} = N_{\psi\phi} = \frac{K(1-\mu)}{2}s^o_{\phi\psi}, \tag{14}$$

$$M_{\phi\phi} = D(k_{\phi\phi} + \mu k_{\psi\psi}), \tag{15}$$

$$M_{\psi\psi} = D(k_{\psi\psi} + \mu k_{\phi\phi}), \tag{16}$$

$$M_{\phi\psi} = M_{\psi\phi} = \frac{D(1-\mu)}{2}k_{\phi\psi}. \tag{17}$$

Note the membrane stiffness $K = Yh/(1-\mu^2)$ and the bending stiffness $D = Yh^3/12(1-\mu^2)$, here Y is Young's Modulus and μ is Poisson's ratio. Since the thin paraboloidal shell has non-constant double curvatures, the fundamental equations are very complicated. For simplicity, different assumptions have been put forward, including the membrane approximation, the bending approximation and the Donnell Mushtari–Vlasov approximation. For flexible membrane paraboloidal shells, the membrane approximation is adopted next.

3. Paraboloidal membrane shells

For thin and flexible shells, the membrane approximation is a common approximation in which all bending components are neglected [16].

$$M_{\phi\phi} = M_{\psi\psi} = M_{\phi\psi} = Q_{\phi 3} = Q_{\psi 3} = 0. \tag{18}$$

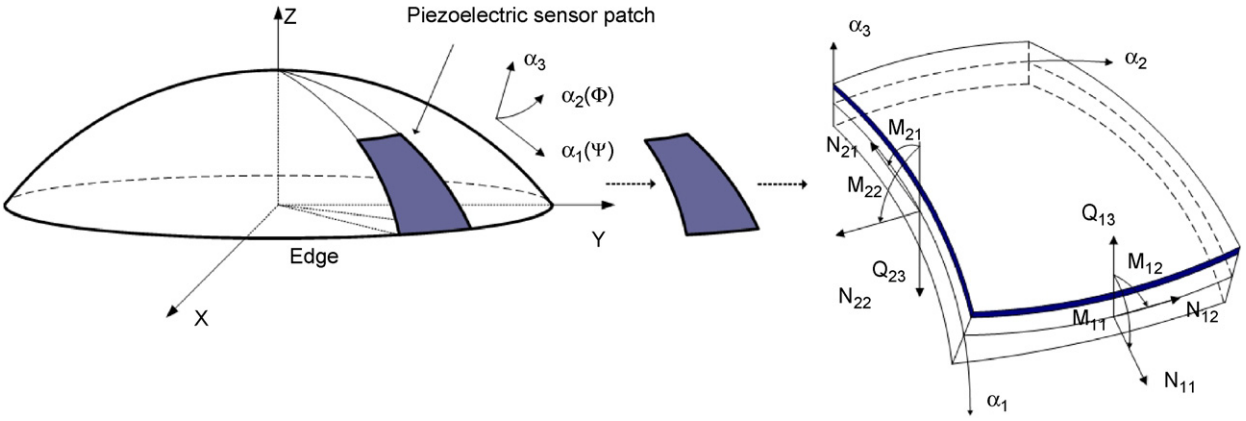

Fig. 2. Stresses of an element of paraboloidal shell with distributed sensor patch.

Table 1
Cases of paraboloidal membrane shells with two different parameters

Case	Parameters	
	Height (c) m	Radius (a) m
1	1	2
2	2	1

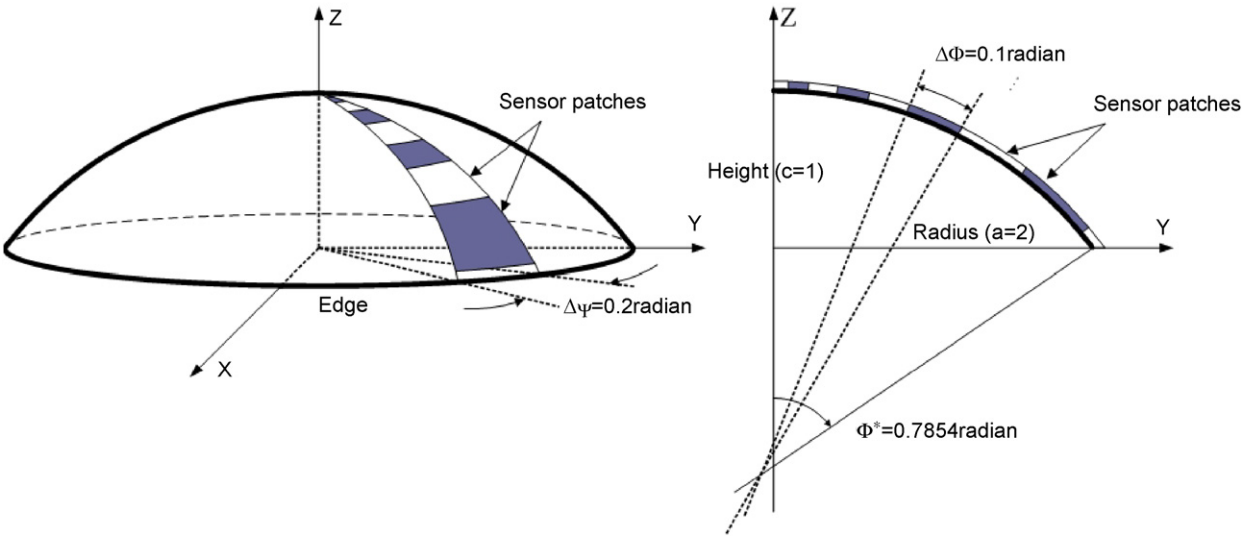

Fig. 3. Sensor patches laminated on the shallow paraboloidal membrane shell (Case 1).

This approximation is also called the extensional approximation and thus the system equations can be derived accordingly:

$$\frac{\partial(R_\psi N_{\phi\phi}\sin\phi)}{\partial\phi} + R_\phi\frac{\partial N_{\psi\phi}}{\partial\psi} - N_{\psi\psi}R_\phi\cos\phi + R_\phi R_\psi\sin\phi F_1 = R_\phi R_\psi\sin\phi\rho h\ddot{u}_\phi, \tag{19}$$

$$\frac{\partial(R_\psi N_{\phi\psi}\sin\phi)}{\partial\phi} + R_\phi\frac{\partial N_{\psi\psi}}{\partial\psi} - N_{\psi\phi}R_\phi\cos\phi + R_\phi R_\psi\sin\phi F_2 = R_\phi R_\psi\sin\phi\rho h\ddot{u}_\psi, \tag{20}$$

$$-R_\phi R_\psi\sin\phi\left(\frac{N_{\phi\phi}}{R_\phi}+\frac{N_{\psi\psi}}{R_\psi}\right) + R_\phi R_\psi\sin\phi F_3 = R_\phi R_\psi\sin\phi\rho h\ddot{u}_3. \tag{21}$$

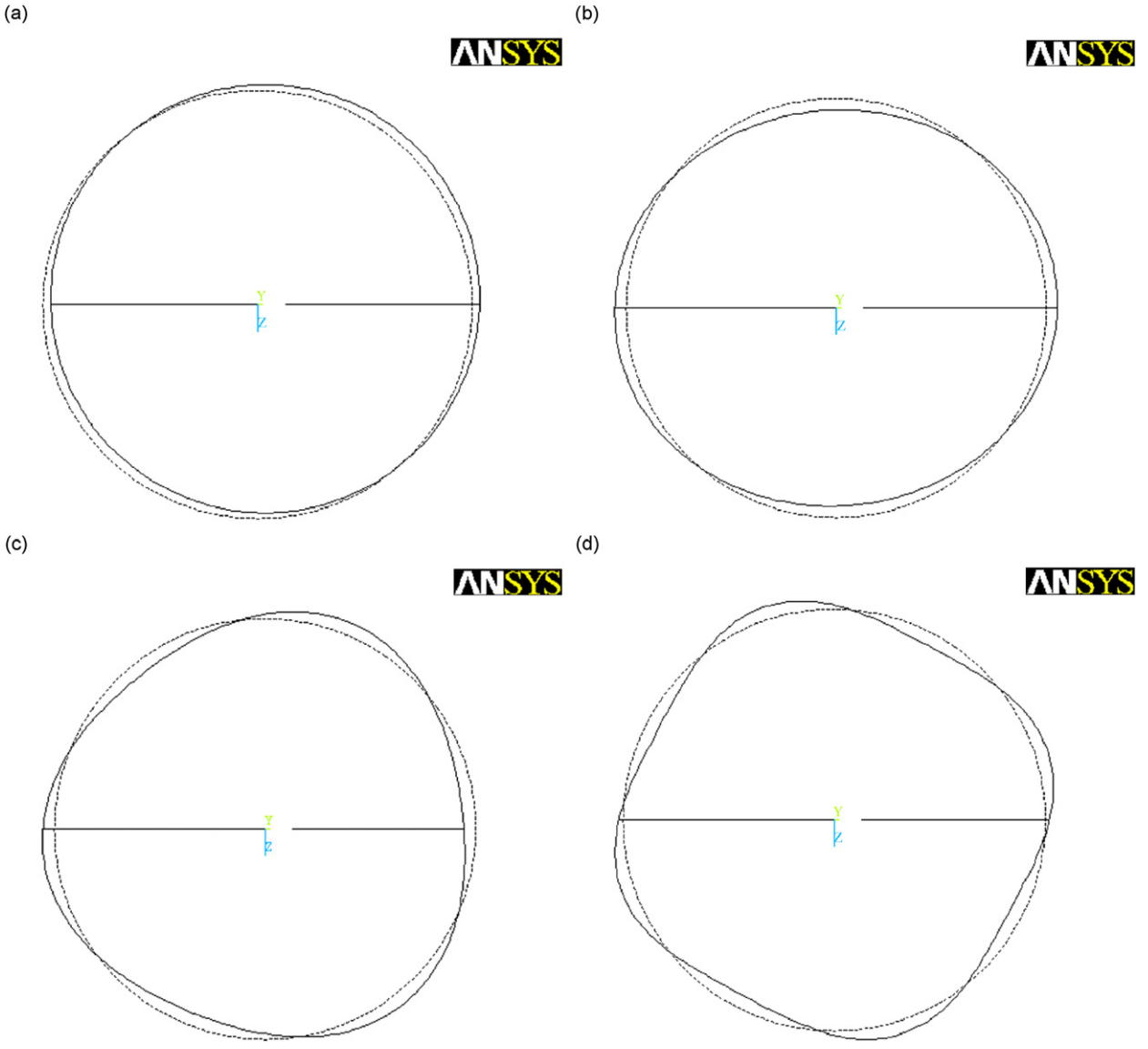

Fig. 4. Free oscillation mode shapes (solid lines) of flexible paraboloidal shells (dash lines), (a–d), respectively, for modes (1–4).

The relationships between membrane forces and membrane strains are defined by Eqs. (12) and (13). With the membrane approximation, the membrane forces become

$$N_{\phi\phi} = K\left\{\frac{\cos^3\phi}{b}\left(\frac{\partial u_\phi}{\partial\phi} + u_3\right) + \mu\frac{\cos\phi}{b\sin\phi}\left(\frac{\partial u_\psi}{\partial\psi} + u_\phi\cos\phi + u_3\sin\phi\right)\right\}, \tag{22}$$

$$N_{\psi\psi} = K\left\{\frac{\cos\phi}{b\sin\phi}\left(\frac{\partial u_\psi}{\partial\psi} + u_\phi\cos\phi + u_3\sin\phi\right) + \mu\frac{\cos^3\phi}{b}\left(\frac{\partial u_\phi}{\partial\phi} + u_3\right)\right\}, \tag{23}$$

$$N_{\phi\psi} = N_{\psi\phi} = \frac{K(1-\mu)}{2}\frac{\cos\phi}{b\sin\phi}\left(\frac{\partial u_\phi}{\partial\psi} + \cos^2\phi\sin\phi\frac{\partial u_\psi}{\partial\phi} - u_\psi\cos\phi\right). \tag{24}$$

For evaluating distributed sensor signals and free oscillation behavior of paraboloidal shells, fundamental structure dynamics of shells need to be investigated.

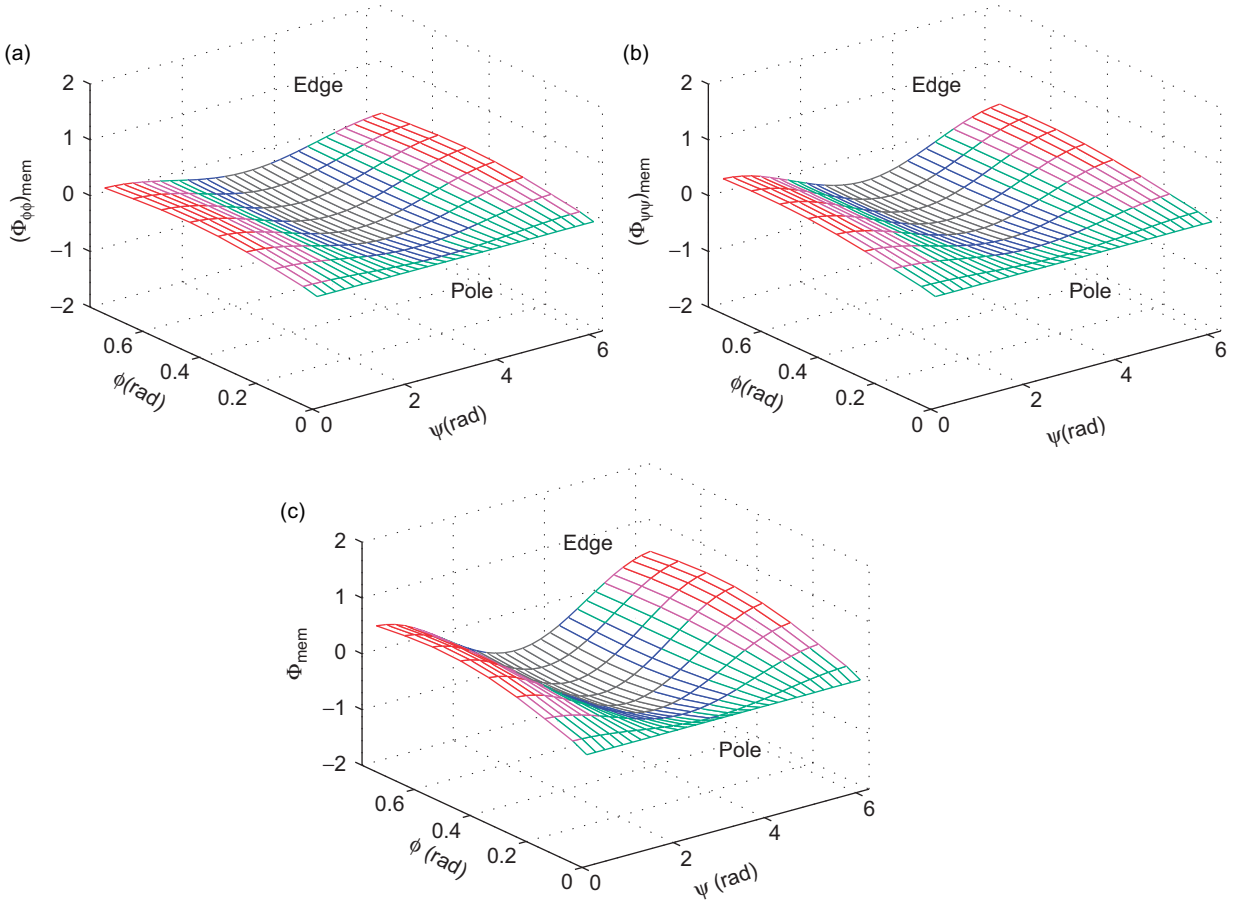

Fig. 5. Sensing signals of shallow shell, when $k = 1$: (a) the meridional sensing signal component; (b) the circumferential sensing signal component; (c) the total distributed sensing signal.

4. Mode shape functions for free-floating paraboloidal membrane shells

Fig. 2 illustrates a paraboloidal shell laminated with a distributed piezoelectric layer and its resultant force and moment distribution of a shell element near the shell edge. Free vibration behaviors of paraboloidal shells are evaluated in this section; distributed sensing characteristics are investigated in the next section.

All external mechanical and electric excitations are zero in free vibration which exhibits shell's intrinsic dynamic characteristics. For a free-floating paraboloidal membrane shell, all forces and moments on the edge are zero, i.e., the displacement and rotation angle are not zero. These boundary conditions (B.C.s) are defined as follows:

$$N_{\phi\phi} = 0, \quad N_{\psi\psi} = 0, \quad Q_{\phi 3} = 0, \quad M_{\phi\phi} = 0. \tag{25}$$

Recall that the membrane approximation requires all moment terms zero, so the mode shape function needs to satisfy the membrane force B.C.s on the boundary. With experienced "trail-and-error" and verification, three new mode shape functions of paraboloidal membrane shells with free B.C are selected as:

$$U_{\phi k} = A_k \cos\frac{(2k+1)\pi}{\phi^*}\phi \sin^{k+1}\phi \cos k\psi, \tag{26a}$$

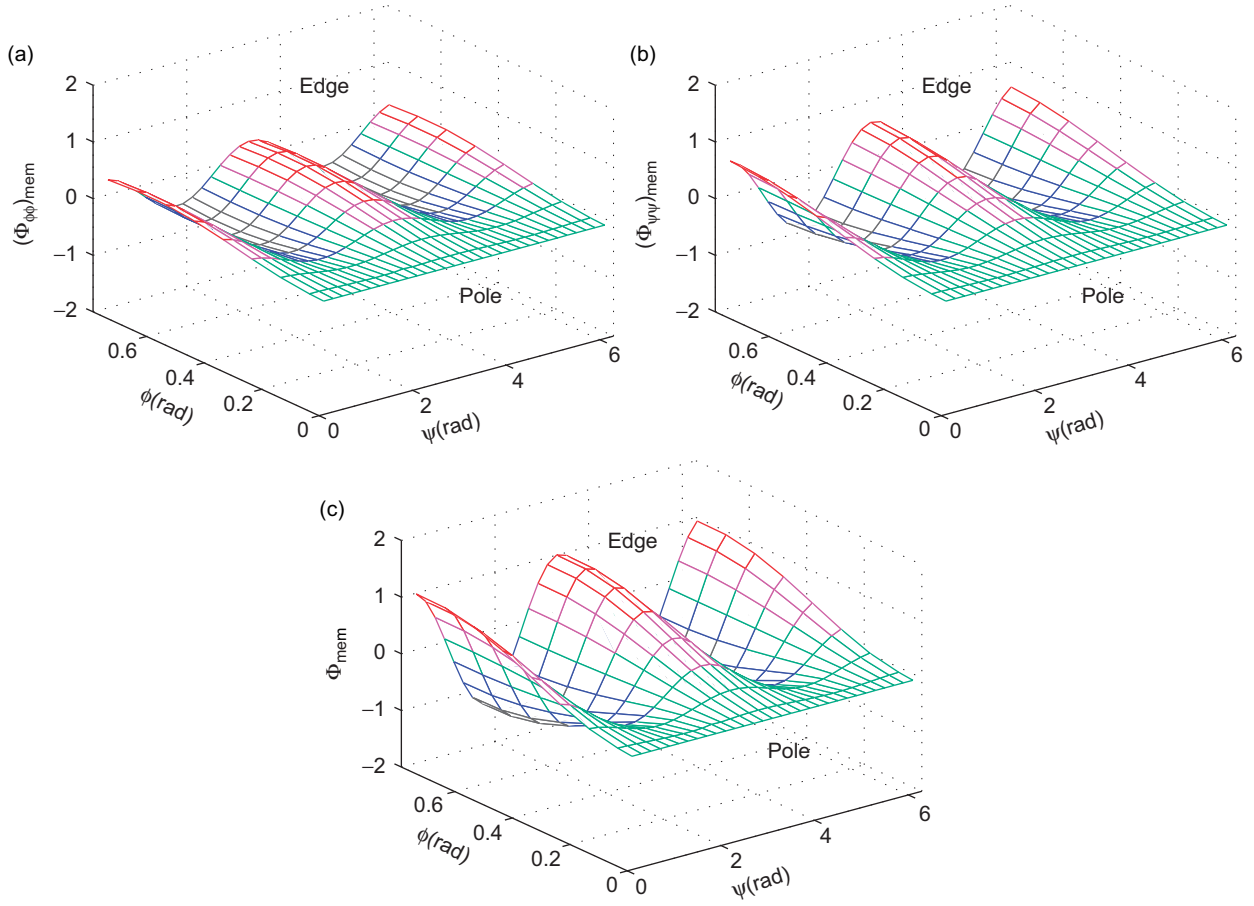

Fig. 6. Sensing signals of shallow shell, when $k = 2$: (a) the meridional sensing signal component; (b) the circumferential sensing signal component; (c) the total distributed sensing signal.

$$U_{\psi k} = -A_k \cos\phi \sin^{k+1}\phi \, \sin k\psi, \tag{26b}$$

$$U_{3k} = A_k(k+1)\cos\phi \sin^{k}\phi \, \cos k\psi. \tag{26c}$$

Here the mode number $k = 1, 2, 3\ldots$, ϕ^* is the meridional boundary angle, ϕ is a meridional variable between $0\sim\phi^*$, and A_k is the kth modal amplitude. The total dynamic response can be represented by the summation of all participating natural modes and their respective modal participation factor:

$$u_i(\phi, \psi, t) = \sum_{k=1}^{\infty} \eta_k(t)\, U_{ik}(\phi, \psi), \quad i = 1, 2, 3. \tag{27}$$

Note $\eta_k(t)$ is the modal participation factor, $U_{ik}(\phi,\psi)$ is the mode shape function, k denotes the kth mode. Distributed signals resulting from segmented piezoelectric sensor patches laminated on paraboloidal shells are discussed next.

5. Distributed sensor signal of paraboloidal membrane shells

Piezoelectric patches spatially distributed on shell surface provide distributed global dynamic signals of elastic paraboloidal shells. For paraboloidal shell, two-dimensional distributed sensors are proposed and output signals from these distributed sensors are evaluated.

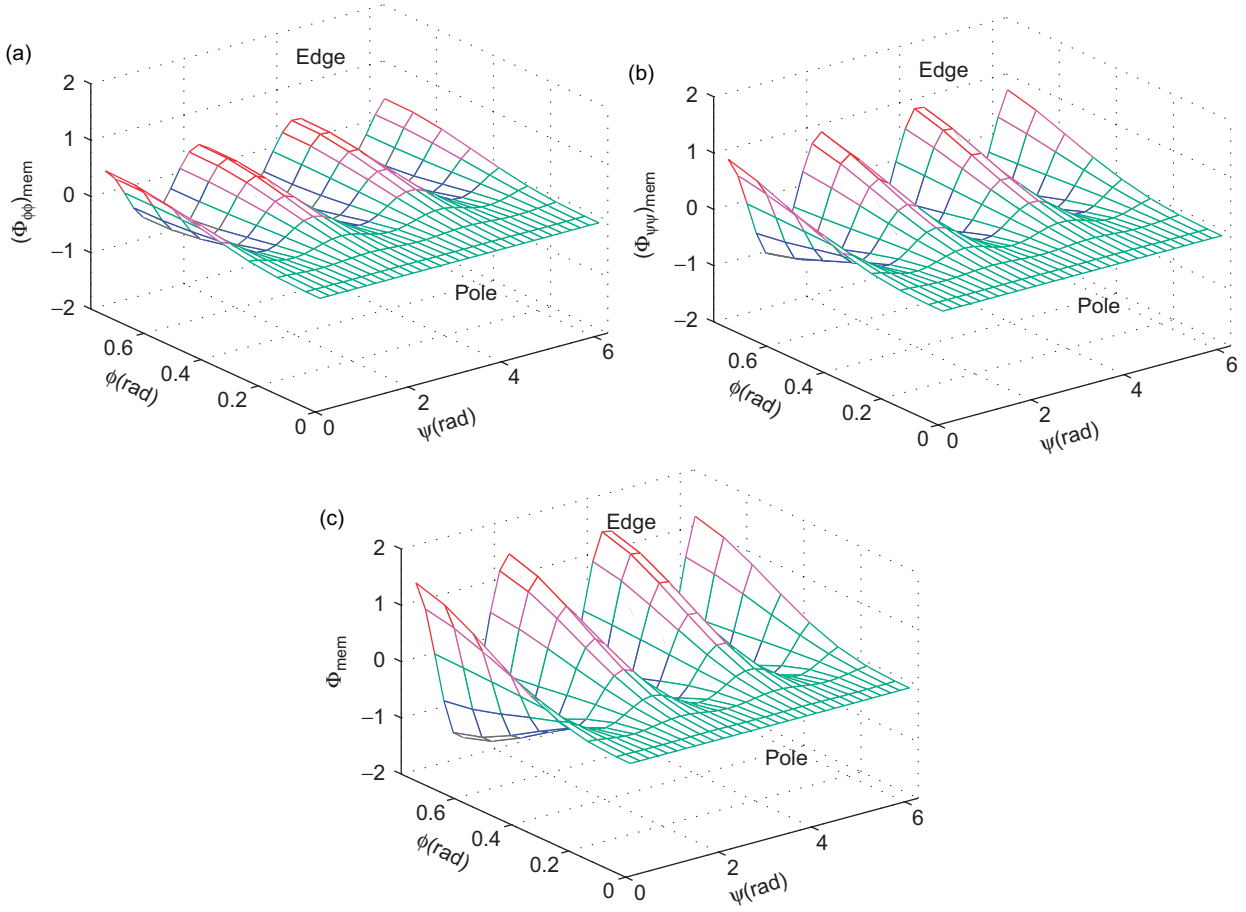

Fig. 7. Sensing signals of shallow shell, when $k = 3$: (a) the meridional sensing signal component; (b) the circumferential sensing signal component; (c) the total distributed sensing signal.

It is assumed that the distributed piezoelectric sensor is uniformly thin, as compare with shell thickness. Thus, the piezoelectric sensor strains are constant and it is equal to the outer surface strains of the paraboloidal shell. It is worth noting that as the distributed sensor, only the direct piezoelectric effect is considered. So one can define an open-circuit voltage ϕ^s in the transverse direction as

$$\phi^s = \frac{h^s}{S^e}\int_{\alpha_1}\int_{\alpha_2}(h_{31}S^s_{11} + h_{32}S^s_{22} + h_{36}S^s_{12})A_1A_2\,\mathrm{d}\alpha_1\,\mathrm{d}\alpha_2, \tag{28}$$

where h^s is the distributed sensor thickness; S^e is the effective sensor electrode area; h_{3i} is the piezoelectric constant indicating a signal generation in the transverse direction due to the strain in the ith direction; S^s_{ij} is the strain on the ith surface in the jth direction. Furthermore, the strain can be divided into the membrane strain and the bending strain, namely $S^s_{ij} = s^o_{ij} + r^s k_{ij}$, here r^s is the sensor location away from the shell neutral surface. Since many piezoelectric materials are not sensitive to in plane shear strain S^s_{12}, the signal expression can be simplified to

$$\phi^s = \frac{h^s}{S^e}\int_{\alpha_1}\int_{\alpha_2}(h_{31}S^s_{11} + h_{32}S^s_{22})A_1A_2\,\mathrm{d}\alpha_1\,\mathrm{d}\alpha_2. \tag{29}$$

For paraboloidal shells, sensor sensitivities can be defined in three principal motions, namely along the meridian, circumferential and transverse directions. For thin membrane shells with free boundary, vibration in the transverse direction dominates and thus it is only considered in this study. Assuming $h_{31} = h_{32}$ and

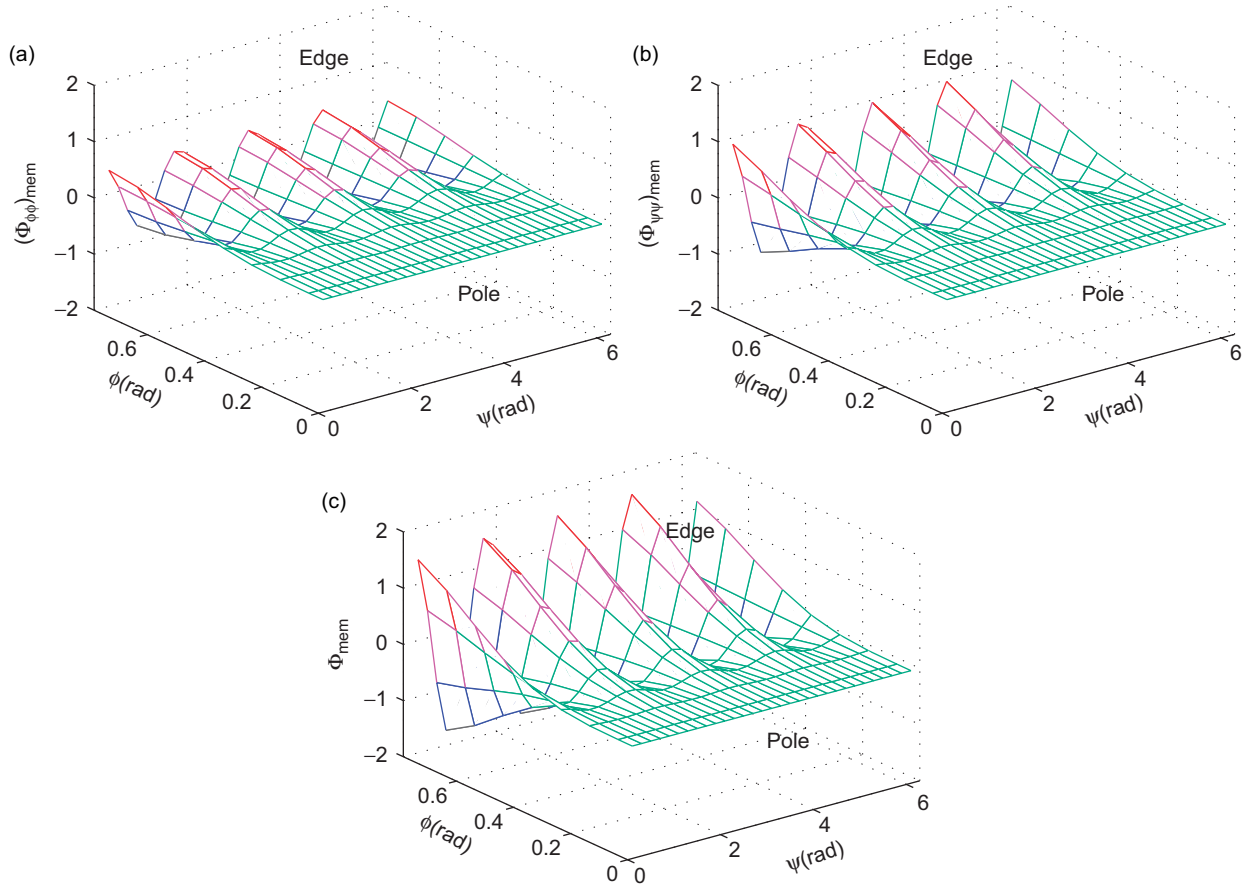

Fig. 8. Sensing signals of shallow shell, when $k = 4$: (a) the meridional sensing signal component; (b) the circumferential sensing signal component; (c) the total distributed sensing signal.

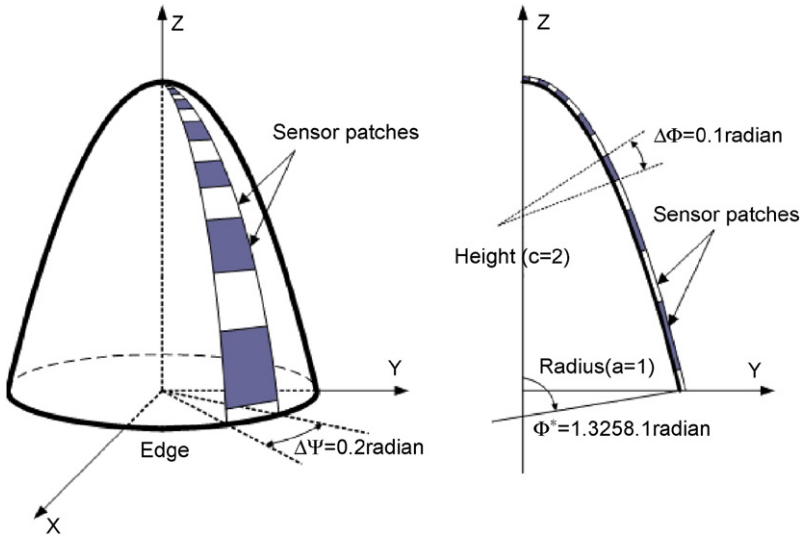

Fig. 9. Sensor patches laminated on a deep paraboloidal membrane shell (Case 2).

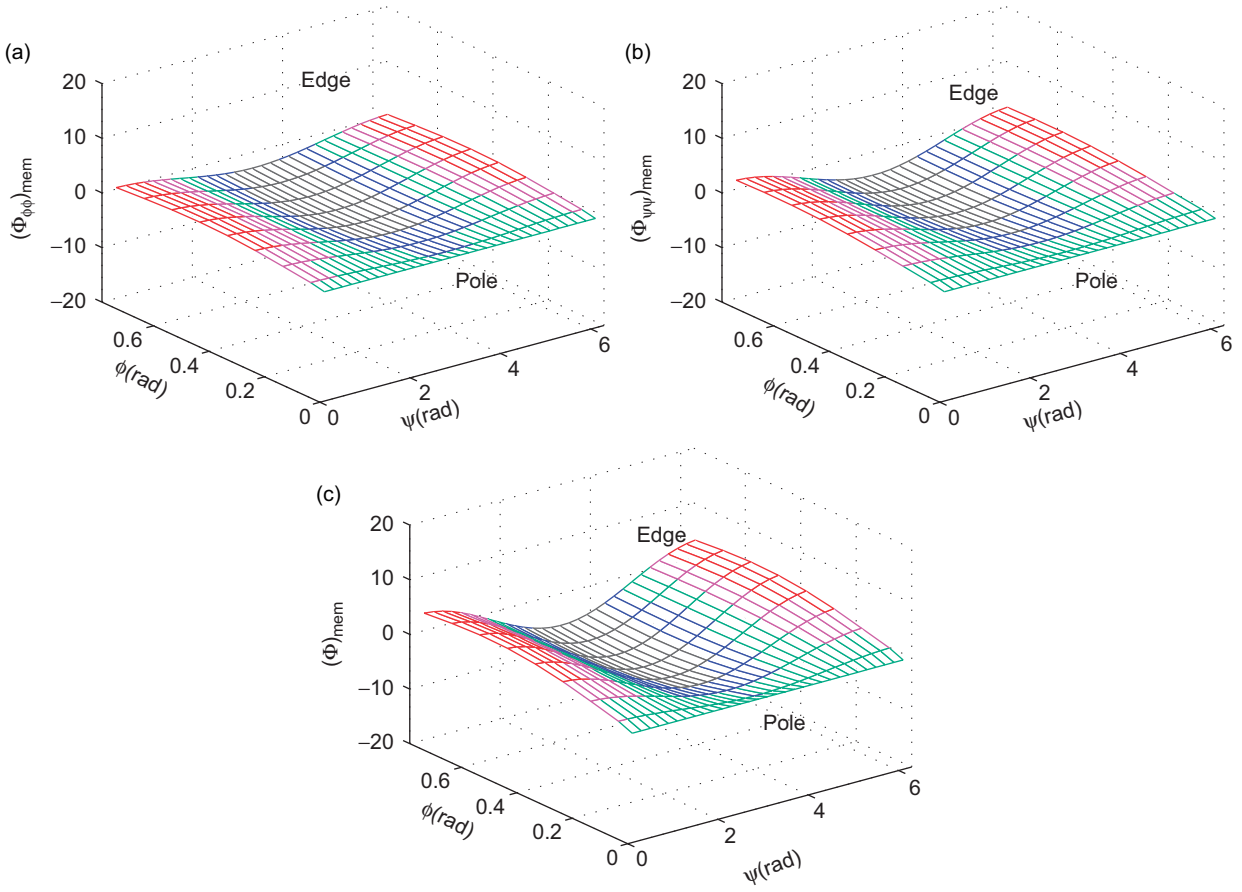

Fig. 10. Sensing signals of deep shell, when $k = 1$: (a) the meridional sensing signal component; (b) the circumferential sensing signal component; (c) the total distributed sensing signal.

substituting mode shape function into the strains, using shell Lamé parameters yields the sensor signal:

$$\begin{aligned}\phi^s &= \frac{h^s}{S^e}\int_{\alpha_1}\int_{\alpha_2}(h_{3\phi}S^s_{\phi\phi}+h_{3\psi}S^s_{\psi\psi})A_1A_2\,\mathrm{d}\alpha_1\,\mathrm{d}\alpha_2\\ &= \frac{h^s h_{3i}}{S^e}\int_{\phi}\int_{\psi} b[(k+1)\sin^{k+1}\phi\cos k\psi+(k+1)\sin^{k+1}\phi\sec^2\phi\cos k\psi]\,\mathrm{d}\phi\,\mathrm{d}\psi\\ &= h^s h_{3i}[(\phi_{\phi\phi})_{\mathrm{mem}}+(\phi_{\psi\psi})_{\mathrm{mem}}],\end{aligned} \tag{30}$$

where $b=a^2/2c$ (as shown in Fig. 1), $(\phi_{\phi\phi})_{\mathrm{mem}}$ and $(\phi_{\psi\psi})_{\mathrm{mem}}$ are, respectively, the meridional and circumferential membrane signal components. Assume an arbitrary distributed sensor is defined by $\phi_1\sim\phi_2$ and $\psi_1\sim\psi_2$, the two signal components $(\phi_{\phi\phi})_{\mathrm{mem}}$ and $(\phi_{\psi\psi})_{\mathrm{mem}}$ are:

$$(\phi_{\phi\phi})_{\mathrm{mem}}=\frac{b(k+1)}{S^e}(\sin k\psi_2-\sin k\psi_1)\int_{\phi_1}^{\phi_2}\sin^{k+1}\phi\,\mathrm{d}\phi, \tag{31}$$

$$(\phi_{\psi\psi})_{\mathrm{mem}}=\frac{b(k+1)}{S^e}(\sin k\psi_2-\sin k\psi_1)\int_{\phi_1}^{\phi_2}\sin^{k+1}\phi\sec^2\phi\,\mathrm{d}\phi, \tag{32}$$

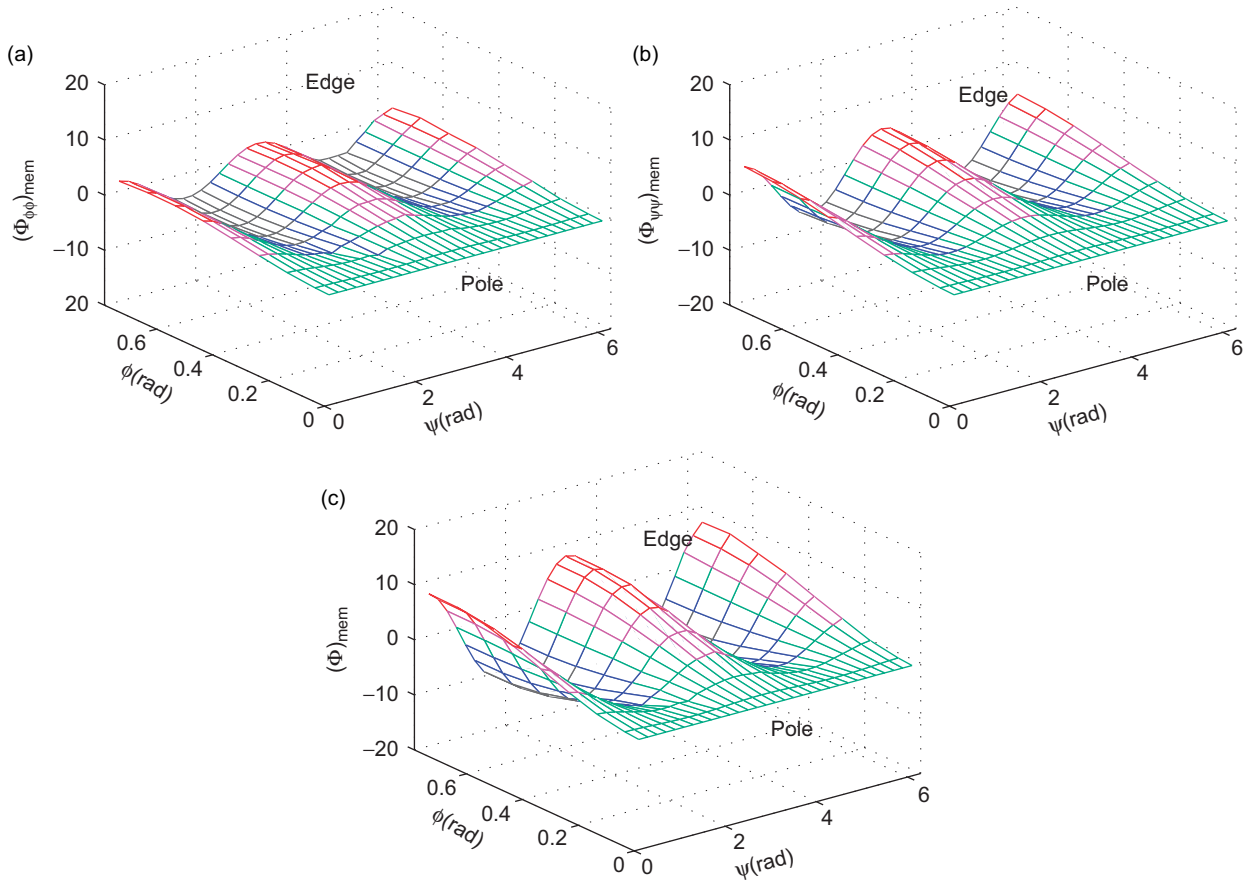

Fig. 11. Sensing signals of deep shell, when $k=2$: (a) the meridional sensing signal component; (b) the circumferential sensing signal component; (c) the total distributed sensing signal.

where

$$S^e = \int_{\phi_1}^{\phi_2}\int_{\psi_1}^{\psi_2} A_1 A_2 \,\mathrm{d}\psi\,\mathrm{d}\phi = \int_{\phi_1}^{\phi_2}\int_{\psi_1}^{\psi_2} \frac{b^2 \sin\phi}{\cos^4\phi}\,\mathrm{d}\psi\,\mathrm{d}\phi = b^2(\psi_2-\psi_1)\frac{\cos^3\phi_1 - \cos^3\phi_2}{3\cos^3\phi_1\cos^3\phi_2}. \tag{33}$$

Accordingly, the microscopic sensing signal components of distributed sensor patches defined by ($\phi_1 \sim \phi_2$) and ($\psi_1 \sim \psi_2$) can be evaluated at different locations. And analysis of sensing signal characteristics and effects of shell geometries can be investigated in case studies.

6. Case studies

For paraboloidal shells, geometric parameters are of importance to shell dynamic characteristics, since both radii of curvatures are non-constant. In this section, the microscopic sensing signal components of flexible membrane paraboloidal shell with different curvatures are evaluated. Two cases are shown in Table 1, in which Case 1 is a shallow paraboloidal shell and Case 2 is a deep paraboloidal shell [15]. The shallow shell is investigated first.

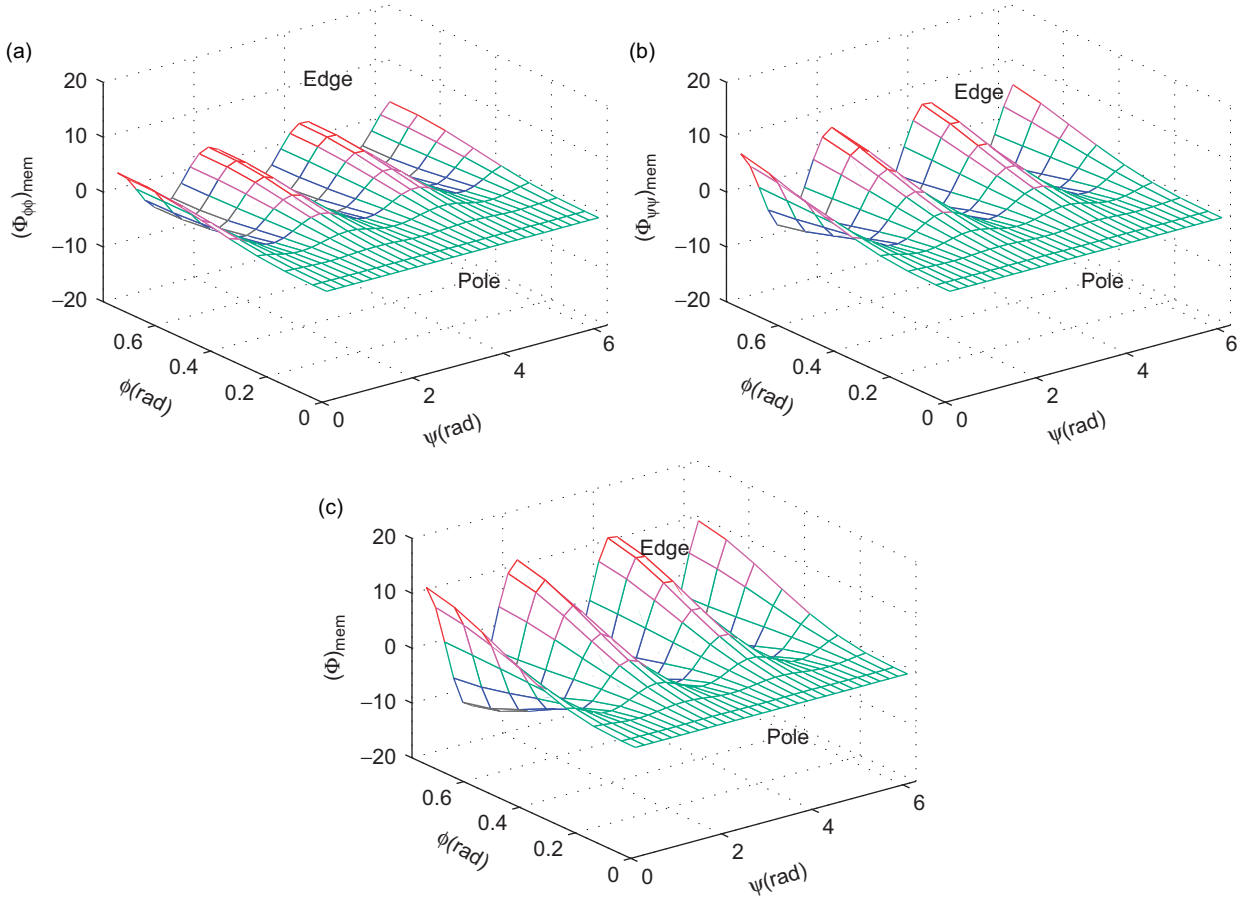

Fig. 12. Sensing signals of deep shell, when $k = 3$: (a) the meridional sensing signal component; (b) the circumferential sensing signal component; (c) the total distributed sensing signal.

6.1. Case 1: Shallow paraboloidal membrane shell

Case 1 is a shallow paraboloidal shell with meridional angle from 0 to 0.7854 radians ($\phi^* = 0.7854$) along the meridional direction and a circumferential angle from 0 to 2π radians ($\psi = 0 \sim 2\pi$) along the circumferential direction, Fig. 3. Free vibration mode shapes are investigated first, followed by distributed sensor signals.

6.1.1. Free vibration mode shapes

Free vibration mode shapes of shallow paraboloidal shell are investigated using the finite element tool—ANSYS. The model is built using *shell 41* element with free B.C. Fig. 4 illustrates the mode shapes of the first four modes.

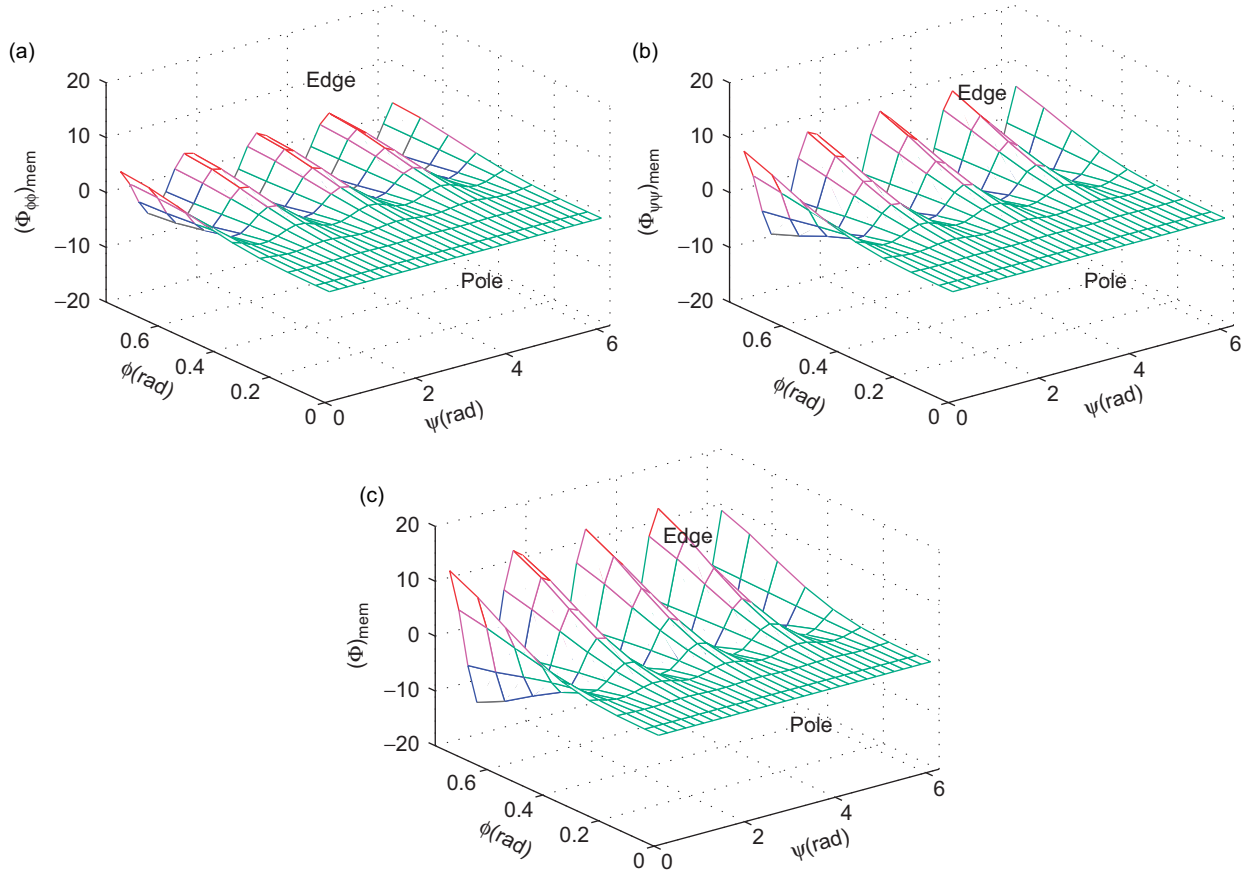

Fig. 13. Sensing signals of deep shell, when $k = 4$: (a) the meridional sensing signal component; (b) the circumferential sensing signal component; (c) the total distributed sensing signal.

Table 2
Comparison of maximal signal magnitudes of two paraboloidal membrane shells (Case 1—shallow; Case 2—deep)

		Mode 1	Mode 2	Mode 3	Mode 4
Case 1 ($c/a = 1/2$)	$(\phi_{\phi\phi})_{mem}$	0.284	0.435	0.536	0.597
	$(\phi_{\psi\psi})_{mem}$	0.381	0.738	0.989	1.103
	$(\phi)_{mem} = (\phi_{\phi\phi})_{mem} + (\phi_{\psi\psi})_{mem}$	0.652	1.138	1.526	1.699
Case 2 ($c/a = 2/1$)	$(\phi_{\phi\phi})_{mem}$	2.273	3.616	4.29	4.777
	$(\phi_{\psi\psi})_{mem}$	3.051	5.902	7.916	8.822
	$(\phi)_{mem} = (\phi_{\phi\phi})_{mem} + (\phi_{\psi\psi})_{mem}$	5.217	9.076	12.206	13.599

6.1.2. Microscopic sensor signals of sensor patches

To evaluate the spatial micro-sensing signal characteristic, the size of distributed sensor patches is defined as: $\Delta\phi = \phi_2 - \phi_1 = 0.1$ rad, $\Delta\psi = \psi_2 - \psi_1 = 0.2$ rad, except patches close to the free edge with $\Delta\phi = \phi_2 - \phi_1 = 0.08$ rad. Thus, there are 248 sensor patches (i.e., 8 patches in the meridional direction and 31 patches in the circumferential direction) laminated on the shallow paraboloidal membrane shell and their sensor areas can be calculated by Eq. (33). Using the sensing signal component expressions defined previously, one can calculate the detail signal components of sensor patches at various locations for different natural modes and those signals, i.e., $(\phi_{\phi\phi})_{\text{mem}}$, $(\phi_{\psi\psi})_{\text{mem}}$ and $(\phi)_{\text{mem}} = (\phi_{\phi\phi})_{\text{mem}} + (\phi_{\psi\psi})_{\text{mem}}$, are, respectively, plotted. Figs. 5–8 illustrate these spatially distributed signal components of the first four modes ($k = 1$ to 4) on shallow paraboloidal membrane shells. The micro-sensing signal is always near to zero (or ≈ 0) at the centre pole and varies with respective to different wavenumbers at the free edge.

With the mode number increasing, the signal wave pattern grows at the free edge corresponding to modal strain variations, and the signal magnitude decreases due to diminishing membrane strains at higher modes, though the modal amplitude A_k assumed unity. In practice, the modal amplitude usually decreases at higher modes, too. Furthermore, the circumferential membrane modal signal component $(\phi_{\psi\psi})_{\text{mem}}$ is larger than the meridional membrane modal signal component $(\phi_{\phi\phi})_{\text{mem}}$. Detailed signal magnitude comparisons of two cases are summarized later.

6.2. Case 2: Deep paraboloidal membrane shell

Case 2 is a deep paraboloidal shell, which is laminated with 13 sensor patches in the meridional direction and 31 patches in the circumferential direction on its surface, as shown in Fig. 9. Spatial micro-sensing signal distribution patterns of Case 2 are very similar to those of Case 1. However, signal magnitudes of distributed sensor of Case 2 are larger than those of Case 1. Figs. 10–13 illustrate the sensing signal distributions of first four modes of deep paraboloidal shell—Case 2.

Modal signal magnitudes of various components of the two cases are summarized in Table 2. Since modal amplitudes are normalized, induced modal strains in deep shell are higher than those of shallow shell. Accordingly, the resulting microscopic signal components of deep shell are higher than those of shallow membrane shell. Again, quantitative comparison indicates the circumferential contribution dominates in all modal signals and the signals gradually decrease at higher modes, due to diminishing influence of membrane effects to higher modes.

7. Conclusions

In this study, mathematical modeling, dynamic characteristics, mode shape functions, micro-sensing signals and signal components with various curvatures of flexible paraboloidal membrane shells were presented. A new set of mode shape functions for free-floating paraboloidal membrane shells were proposed and used in the distributed signal analysis. Based on detailed analysis of micro-sensing signals of paraboloidal membrane shells, the following conclusions can be drawn:

(1) For thin and flexible paraboloidal membrane shells, the membrane approximation was adopted in this study. Thus, distributed sensing signals are dominated by membrane strains, while components resulting from bending strains are all zeros. Quantitative comparison indicates the circumferential component dominates in all modal signals and the signals gradually decrease at higher modes, due to diminishing influence of membrane effects to higher modes.
(2) Micro-sensing signal of the sensor patches differs at various locations and modes on paraboloidal shells. Signal is zero at the pole; it fluctuates with the change of wavenumbers at the free boundary in accordance with modal dynamic behaviors. Natural modal strain variations of thin paraboloidal shells generate distributed sensor signals in sensor patches, which are distinct among shell natural modes.
(3) Contribution of circumferential membrane signal component is larger than that of meridional membrane signal component in overall sensing signal for a given mode, although the difference between the two components is not significant in this study.

(4) The curvature of paraboloidal shells influences micro-sensing signal amplitudes of piezoelectric distributed sensor patches. Although the micro-sensing signal patterns are similar among membrane shells with various curvatures, signals magnitudes of deep membrane paraboloidal shell are larger than those of shallow shell.

Based on the detailed microscopic sensing signal analysis, design guidelines of optimal sensor placements can be assured. Spatially distributed signals are location and modal dependent. Depending on user's application, one can selectively place sensor patch(es) at critically locations to maximize the output at the minimal cost. These data are also valuable to develop dynamic vibration control and static shape actuation of lightweight paraboloidal flexible structures ranging from micro-electromechanical systems to large-scale space structures.

Acknowledgements

This research is supported, in part, by a grant from the Spaceflight Technical Innovation Foundation of China (HTCX2005-01) and the National Natural Science Foundation of China (No. 50675043). Prof. Tzou also likes to thank the Visiting Professorship program and the 111 Project (B07018) at the Harbin Institute of Technology.

References

[1] E.F. Crawley, Intelligent structures for aerospace: a technology overview and assessment, *AIAA Journal* 32 (8) (1994) 1689–1699.
[2] C.A. Rogers, Intelligent material system—the dawn of a new materials age, *Journal of Intelligent Material System and Structures* 4 (1993) 4–12.
[3] U. Gabbert, H.S. Tzou, *Smart Structures and Structronic System*, Kluwer Academic Publishers, Dordrecht, Boston, London, 2001.
[4] H.S. Tzou, G.L. Anderson, (Eds.), *Intelligent Structural System,* Kluwer Academic Publishers, Dordrecht, Boston, London, 1992.
[5] J. Callahan, H. Baruh, Modal sensing of circular cylinder shells using segmented piezoelectric elements, *Smart Material and Structures* 8 (1999) 125–135.
[6] H.-R. Shih, R. Smith, Photonic control of cylindrical shells with electro-optic photostrictive actuators, *AIAA Journal* 42 (2) (2004) 341–347.
[7] H.S. Tzou, *Piezoelectric Shells (Distributed Sensing and Control of Continua)*, Kluwer Academic Publishers, Boston, Dordrecht, 1993.
[8] H.S. Tzou, J.P. Zhong, J.J. Hollkamp, Spatially distributed orthogonal piezoelectric shell actuators (theory and applications), *Journal of Sound and Vibration* 177 (3) (1994) 363–378.
[9] J. Qiu, J. Tani, Vibration control of a cylindrical shell using distributed piezoelectric sensors and actuators, *Journal of Intelligent Material Systems and Structures* 6 (4) (1995) 474–481.
[10] A.R. Faria, S.F.M. Almeida, Axisymmetric actuation of composite cylindrical thin shells with piezoelectric rings, *Smart Materials and Structures* 7 (6) (1998) 843–850.
[11] V. Birmax, G.J. Knowles, J.J. Murray, Application of piezoelectric actuators to active control of composite spherical caps, *Smart Materials and Structures* 8 (1999) 128–222.
[12] H.S. Tzou, D.W. Wang, W.K. Chai, Dynamics and distributed control of conical shells laminated with full and diagonal actuators, *Journal of Sound and Vibration* 256 (1) (2002) 65–79.
[13] H.S. Tzou, D.W. Wang, Micro-sensing characteristics and modal voltages of piezoelectric laminated linear and nonlinear toroidal shells, *Journal of Sound and Vibration* 254 (2) (2002) 203–218.
[14] H.S. Tzou, P. Smithmaitrie, J.H. Ding, Sensor electromechanics and distributed signal analysis of piezoelectric-elastic spherical shells, *Mechanical System and Signal Processing* 16 (2/3) (2002) 185–199.
[15] J.H. Ding, H.S. Tzou, Micro-electromechanics of sensor patches on free paraboloidal shell structronic systems, *Mechanical System and Signal Processing* 18 (2004) 367–380.
[16] W. Soedel, *Vibrations of Shell and Plates*, Material Dekker Inc., New York, 1981.